

Masterarbeit

Pressure Gradient and Geometrical Variation of the Abrasive Blocks during the Polishing Process of Ceramic Tiles with Line Contact

von Cand. M.Sc. Amiril Sahab Abdul Sani

Matr.-Nr. 387954

Betreuer:

Jun. Prof. Dr.-Ing. Balázs Magyar

Apl. Prof. Dr. Eng. Fábio J.P. Sousa

September 2014

Abstract

A series of experimental investigation has been carried out to develop and describe the distribution of pressure gradient underneath and across the topological surface of laboratory grinding tools. The surface pressure plays a key role during polishing process of ceramic tiles in gloss gaining and development of surface roughness.

Analogous to the surface topography changes of the grinding tools and ceramic tiles, the wear of the work tools and work pieces are proportional to the grinding work that was performed between the surfaces during the polishing process.

The present work intends to evaluate the influence of the gradual distribution of surface pressure in polishing ceramic tiles with line contact. For this purpose, two grinding tools were assembled together as a polishing head and installed on a CNC tribometer machine with a deflection angle of 2.2° from the base coordinate system of the machine.

In this thesis, the theory of pressure distributed gradually underneath and across the polishing tools was successfully defined by implementing a new polishing tool composed of rotating shaft with pivot joint, helical springs and two abrasive blocks attached on it.

These findings enhance the understanding of pressure distribution from previous study of polishing with flat contact using single abrasive block. With these comparisons the process outcome in terms of gloss level and fine surface finish could be further optimised. The effect of the material removal and gloss development due to polishing tools configuration with preferred process parameters were found to be minimised or maximised according to the kinematics chosen. Differences were clearly illustrated at the end of the work.

Table of Content

Acknowledgement	I
Abstract	II
Table of Content	III
List of Figures	V
List of Tables	VIII
Nomenclature	IX
Abbreviation	XI
1 Overview	1
1.1 <i>Introduction</i>	1
1.2 <i>Assignment of task</i>	2
2 State of the Art	3
2.1 <i>Honing or polishing ceramic tiles</i>	3
2.2 <i>Grinding work during polishing</i>	5
2.3 <i>Spring moment during polishing</i>	8
2.4 <i>Contact Pressure during polishing</i>	13
3 Experiments	18
3.1 <i>Preparation of grinding tools</i>	18
3.2 <i>Preparation of sample work piece</i>	21
3.3 <i>Test rig setup</i>	22
4 Approaches	23
4.1 <i>First experiment – Surface preparation of fickers</i>	23
4.2 <i>Second experiment – Rotation with pressure gradient</i>	25
4.3 <i>Third experiment – Rotation without pressure gradient</i>	26
4.4 <i>Data acquisition</i>	27

5	Results and Discussion.....	34
5.1	<i>First experiment – Surface development of fickerts.....</i>	34
5.2	<i>Second experiment – Rotation with helical springs</i>	41
5.3	<i>Third experiment – Rotation without helical springs</i>	45
5.4	<i>Data comparison.....</i>	50
6	Conclusions and Recommendations	54
	References	56
	Attachment	58

List of Figures

Figure 2-1: Schematic diagrams of: (a) a rotating tangential grinding head with two abrasive blocks attached on it and a ceramic tile transported slowly beneath the head (adapted from Cantavella [Cant04]) and (b) a fickert in contact with the tile [Hutc05b]	6
Figure 2-2: Model of the polishing tools, the rotating axis and the corresponding velocity gradient during the polishing process.	7
Figure 2-3: Tribometer machine available in the laboratory for the experiments	8
Figure 2-4: Polishing tool in laboratory setup; Right: schematic drawing of the tool.....	9
Figure 2-5: Polishing tool (a) at rest and (b) during motion.....	10
Figure 2-6: Sketch of a loading diagram on the polishing tool and the after effect of abraded surface on the ceramic tile.....	11
Figure 2-7: Schematic loading diagram of a polishing tool in static state	11
Figure 2-8: Inclination angle of the spring with (a) inclination angle of the abrasive block and (b) inclination angle of the ceramic tile.....	13
Figure 2-9: Loading diagram of the abrasive block in 2D and its equivalence.....	14
Figure 2-10: Loading diagram exerted by the helical springs; Right: Surface load in 3D	15
Figure 2-11: Moments at pivot joint and resultant forces acting on the abrasive block due to spring pressure	16
Figure 3-1: The cutting process of the fresh fickerts	18
Figure 3-2: Polishing tool with a sample abrasive block fixed on its holder.....	19
Figure 3-3: Polishing head with two polishing tools with exaggerated deflection angle. Left: Deflection of the polishing head; Right: Deflection of a polishing tool.....	19
Figure 3-4: Illustration of a single fickert, which oscillates in a small arc with radius R about a horizontal axis while the whole polishing head rotates about a vertical axis [Hutc05b].....	20
Figure 3-5: Hertzian contact pressure and contact width, 2b as a function of the radius R of the abrasive block during industrial polishing process [Hutc04]	21
Figure 3-6: Installation of inclined armatures on the tribometer	22
Figure 4-1: Kinematics of polishing process in first methodology	24
Figure 4-2: Kinematics of the polishing process in second methodology. Right: Example of 'Black Onix' tile with dimension	25
Figure 4-3: Experimental cycles	26
Figure 4-4: Measuring points of an abrasive block under CMM.....	27
Figure 4-5: Predefined coordinate system on the tool holder for topography measurement of the abraded abrasive's surface	28

Figure 4-6: Schematic diagram of an abrasive block measured under CMM	2
Figure 4-7: Trigonometric function of a triangle	2
Figure 4-8: Example of a data process in LabVIEW of abrasive block topography	2
Figure 4-9: Measuring points of a ceramic tile sample with CMM.....	3
Figure 4-10: Predefined coordinate system on the ceramic tile for topography measurement of the machined surface.....	3
Figure 4-11: Example of a data process in LabVIEW of ceramic tile topography	3
Figure 4-12: Grid size for gloss measurement.....	3
Figure 4-13: Illustration of the gloss measurement [Huan02].....	3
Figure 4-14: Illustration of the grid size on tile surface; Right: A transparent plastic stencil with the measurement sequence	3
Figure 5-1: Illustration of polishing head at initial state against ceramic tile S1 in first experiment.....	3
Figure 5-2: Evolution of inclination angle and its wear of an abraded abrasive blocks from #320 until #Lux of first polishing tool, A01.....	3
Figure 5-3: Evolution of inclination angle and its wear of an abraded abrasive blocks from #320 until #Lux of second polishing tool, A02	3
Figure 5-4: Spring pressures exerted by abrasive block A-01 for all six abrasive mesh sizes.....	3
Figure 5-5: Spring pressures exerted by abrasive block A-02 for all six abrasive mesh sizes.....	3
Figure 5-6: Evolution of average curvature radius in the cross sectional area of the first abrasive block, A01	4
Figure 5-7: Evolution of average curvature radius in the cross sectional area of the second abrasive block, A02	4
Figure 5-8: Illustration of polishing head against ceramic tile S2 in second experiment.....	4
Figure 5-9: Evolution of inclination angle and its height of an abraded abrasive block A01, from #32 until #Lux after polishing of Sample 2.....	4
Figure 5-10: Evolution of inclination angle and its height of an abraded abrasive block A02, from #32 until #Lux after polishing of Sample 2.....	4
Figure 5-11: Average depth of machined surface measured from the tile centre – S2	4
Figure 5-12: Average Gloss Unit measured in direction tangential to the tile's radius of S2.....	4
Figure 5-13: Average surface roughness measured from inner to outer side of the machined surface of S2.....	4
Figure 5-14: Illustration of polishing head without presence of helical springs in third experiment.....	4
Figure 5-15: Evolution of inclination angle and its height of an abraded abrasive block A01, from #32 until #Lux after polishing of Sample 3.....	4

Figure 5-16: Evolution of inclination angle and its height of an abraded abrasive block A02, from #320 until #Lux after polishing of Sample 3.....	47
Figure 5-17: Average depth of machined surface measured from the tile centre – S3	48
Figure 5-18: Average Gloss Unit measured in direction tangential to the tile's radius of S3	48
Figure 5-19: Average surface roughness measured from inner to outer side of the machined surface of S3.....	49
Figure 5-20: Correlation between average glossiness values and roughness profiles	49
Figure 5-21: Scratching score and the development of gloss on S2; Right: Evenly distributed gloss development on S3.....	50

List of Tables

Table 1: Adaptation of process parameters from industrial scale to the laboratory-scale [Olen13a]	2
Table 2: Laboratory parameters for the polishing process.....	2
Table 3: Data of polishing Sample 1 – A01	3
Table 4: Data of polishing Sample 1 – A02	3
Table 5: Data of polishing Sample 2 – A01	4
Table 6: Data of polishing Sample 2 – A02	4
Table 7: Data of polishing Sample 3 – A01	4
Table 8: Data of polishing Sample 3 – A02	4
Table 9: Average gloss measured tangential to the radial distance from tile centre – S2 (line contact)	5
Table 10: Average gloss measured tangential to the radial distance from tile centre – S2 (flat contact)	5
Table 11: Average gloss measured tangential to the radial distance from tile centre for both experiments of polishing with line and flat contact	5
Table 12: Comparison of two sample results between polishing with flat and line contact (gradual pressure distribution).....	5
Table 13: Comparison of two sample results between polishing with flat and line contact (uniform pressure distribution).....	5

Nomenclature

Symbol	Description	Unit
A_N	Contact surface area normal to the applied force	mm ²
b	Contact width between two isotropic bodies in Hertzian contact pressure	mm
c_{Spring}	Spring constant	N/mm
d	Inner diameter of the polishing tool	mm
D	Outer diameter of the polishing tool	mm
F_{Grad}	Gradual line load equivalent to volume of surface pressure	N
F_L	Line load proportional to the Hertzian contact pressure	N/mm
F_N	Applied load or normal force	N
F_{S1}, F_{S2}	Spring forces	N
F_{Spring}	Spring resultant force	N
Δh	Spring displacement	mm
l	Total length of 12 measuring points in a column on fickert surface	mm
L	Distance between two spring centres	mm
$L_{Abrasive}$	Length of the abrasive block	mm
M_{Grad}	Moment at hinge joint due to gradual line load	Nmm
M_{Spring}	Moment acting on the hinge joint due to spring resultant force	Nmm
n_{abr}	Number of abrasives	
N_C	Number of abrasive contacts per passage	-
p	maximum Hertzian contact pressure of elastic bodies	MPa
P_{Max}	Maximum contact pressure between contacts of fickert and tile	N/mm ²
P_{Min}	Minimum contact pressure between contacts of fickert and tile	N/mm ²
P_N	Normal surface pressure	MPa
R	Curvature radius of the abrasive block	mm

R_a	Arithmetic average of the absolute values of the roughness profiles ordinate	μm
r	Distance from the centre of the grinding head to the fickert element	mm
s	Scratching distance of a fickert element	mm
v_{ex}	Speed of the abrasive at outer peripheral	mm/s
v_f	Feed rate of the work piece	mm/s
v_{in}	Speed of the abrasive at inner peripheral	mm/s
v_r	Forward speed relative to radial distance	mm/s
V_{Grad}	Volume of surface pressure equivalent to the gradual line load	MPa*mm ²
$W_{Abrab.}$	Height of fickert's abraded surface	mm
W_{Tile}	Height of tile's abraded surface	mm
$d\dot{W}$	Power or work performed per unit time by the polishing process	Nm/s or J/s
W_{Total}	Total grinding work performed during polishing work	Nm or Joule
Z_i	Coordinate points of abraded surface in Z-axis measured by CMM	mm
$\alpha_{Abrasive}$	Inclination angle of a slope due to wear on an abrasive surface	°
α_{Spring}	Total inclination angle of tools's holder due to spring displacement	°
α_{Tile}	Inclination angle of a slope due to wear on a tile surface	°
μ	Coefficient of friction between fickert and tile surface	-
ω	Rotation speed of polishing tool	rad/s or rpm

General Rules:

Differentiation with respect to time is symbolized by superscript dots

$$\dot{y} = \frac{dy}{dt}, \ddot{y} = \frac{d^2 y(t)}{dt^2}$$

Abbreviation

CAD	Computer Aided Design
CMM	Coordinate Measuring Machine
CNC	Computerized Numerically Controlled
DCC	Direct Computer Control
EXCEL	Microsoft Office spreadsheet software
FEPA	Federation of European Producers of Abrasives
LabVIEW	Laboratory Virtual Instrument Engineering Workbench by National Instruments
MATLAB	Matrix Laboratory by MathWorks
NI-DAQ	National Instrument - Data Acquisition (Device)
NS	National School
PC-DMIS	Personal Computer - Dimensional Measuring Interface Standard
RPM	Revolutions per minute
VI	Virtual Instrument

1 Overview

1.1 Introduction

Porcelain tiles are ceramic material made by heating materials like clay in the form of kaolin, feldspar and sand in a kiln (furnace). Porcelain ceramic products were baked at high temperatures to achieve vitreous qualities such as translucence in the form of gloss and low porosity [Wang03]. Porcelain comes in both glazed and unglazed varieties, fired at a high temperature, representing the most popular unglazed variety. The latter is being widely manufactured in Europe for industrial and architectural usage. The quality of porcelain in mechanical strength and chemical resistance is the essential properties of the extremely low porosity of the ceramic material. Porcelain ceramic tiles are highly resistant to chemical substances and cleaning agents making them extremely serviceable for excellent outdoor flooring and wall cladding in multiple environments [Bert07].

The treated surface finish of porcelain ceramic tile is very versatile and it has a universal application to such degree that its mechanical and aesthetic values by increasing its brilliance and elegance have made them an excellent choice for a wide variety of applications especially in architecture. The good mechanical strength as well as scratch, chemical, stains and frost resistances are the main attractive properties of highly polished unglazed porcelain ceramic tiles.

Polishing, in the other hand, in manufacturing technology's point of view is the production of surfaces with small depth of roughness and certain shape and size allowances. Fine loose granules are rubbed against the workpiece using a soft counterpart to smoothen the surface of the workpiece without changing its nominal mass, dimension or shape. It is understood through definition, that the manufacturing process in gloss gaining and surface finishing of ceramic tiles lie in the area of honing. It is not to be confused with polishing of ceramic tiles because of the continuous usage of the term "polishing" found in literatures, research and scientific papers of manufacturing technology [Olen14].

Surface finish of ceramic tiles can be achieved through following machining treatment: grinding, honing, lapping and polishing under the same standard of machining of geometrically undefined cutting edges according to DIN 8589 [Kloc05]. The utmost difference between these processes is the number of contact between the abrasive particles and the treated surfaces in a period of time.

The task of this thesis work is to enhance the previous study on the development of pressure gradient beneath and across the flat surface of the polishing tool. The experiments were carried out in a custom made test rig built in laboratory scale to match the industrial ceramic polishing processes. By maintaining the same procedures and a few alterations of the parameters to achieve the same output and results, this work has been executed with two polishing tools attached on the polishing head. The contact area between the abrasives and ceramic tiles during polishing was found out to be linear with small width of about 0.2 mm [Hutc05b]. The linear surface pressure calculated in current work will be greater compared to previous polishing process with flat surface [Sani14].

A considerable amount of literature has been published on the distribution of surface pressure produced by contact fretting between surfaces of ceramic tile and polishing tools. However, a better understanding of the treatment in polishing ceramic tiles is still necessary for an optimum understanding of this topic. This will further improve the quality and quantity not only in the total cost of manufacturing ceramic tiles but also in reducing excessive numbers of waste and rejected final products. [Hut05b]

1.2 Assignment of task

The aim of this work is to study and develop the theoretical understanding of the pressure distribution underneath and across the polishing head during polishing of ceramic tiles with grinding tools in line contact. The pressure was reported by researchers to be inconstant along the polishing tools due to kinematics and geometrical structures of the polishing system [Nasc14]. Recent evidence suggests that wear on the polishing tools (abrasives) is inconstant along the polishing tools due to the work done during the polishing motion [Sani14]. The relationship between pressure distribution and wear on contact areas is investigated in this work and the process outcomes are discussed as the work progresses.

It is currently possible to construct or redesign an experimental model of polishing ceramic tile in an early phase before production with the aid of computer aided engineering and design. The study of geometric changes due to wear and work done during polishing requires a mathematical approach to describe and explain the interesting phenomenon of the tribological interactions in polishing process. Moreover, it is much easier and faster to compare different models in the design construction phase with each other directly without interrupting the industrial processes.

For developing the experimental methods, various software and hardware products available for researchers should be optimally integrated with each other. This includes LabVIEW and EXCEL Spreadsheet, for describing the results outcome; Micro-Hite 3D DCC NS Coordinate Measuring Machine (CMM) by TESA for measuring tile surface topography; MarSurf M 300 mobile roughness measurement device by Mahr for determining surface roughness; ZGM 1120 glossiness measurement device by Zehntner to measure the gloss unit; and a custom made CNC-tribometer for the machining works which imitated the industrial polishing machine [Olen13a]. In the end, a constructive comparison method between grinding tools polishing with flat and line contacts is discussed in terms of glossiness and surface wear.

2 State of the Art

2.1 Honing or polishing ceramic tiles

During the past 30 years much more information has become available on the manufacturing of ceramic tiles and their end product finishes [Sánc10]. Honing process, in the manufacturing technology point of view, is the actual final treatment on the ceramic tiles for high gloss achievement and fine surface. The process of honing or polishing ceramic tiles suggested that, ceramic tiles were brought through the industrial polishing line and multiple scratches had been carried out by a sequence of polishing heads with decreasing abrasive particle sizes, known as polishing trains. [Sous13a]

Previous studies have reported that 30 – 40% of the manufacturing costs of ceramic tiles lie in the gloss gaining process [Sous07a]. In 2005, Hutchings et al. reported that more than 40% of the total cost accounted to polishing process alone [Hutc05a]. The current industrial polishing of ceramic tiles has shown a large amount of production waste, excessive numbers of rejected products which resulted in high polishing costs and low productivity [Hutc05b].

The research to date has tended to focus on the influence of pressure gradient and its relative motion on the development of gloss and surface finish. So far, from tests carried out elsewhere [Hutc05b], a sequence of progressively smaller silicon carbide abrasive particles showed a general trend of decreasing roughness and increasing gloss during the polishing process. A previous study by author had also suggested that polishing of ceramic tiles in a series of different grain sizes of single abrasives with flat contact on a single porcelain ceramic tile had a significant effect on gloss gaining and fine surface finish where pressure is at the peak value [Sani14]. The surface wear of both abrasive blocks and ceramic tiles are also affected due to the complex tribological interactions between those contact surfaces.

In addition, the research is intended to produce controlled study which compares differences in parameters used during polishing ceramic tiles found in industrial practises. This method includes the radial gradient of the contact pressure and the scratching speed; tool load which is constant throughout the experiments; tool curvature to create line contact between abrasives and ceramic tiles; and other parameters of the process which are kept constant.

Table below shows the process parameters that are kept constant during the experiments and adaptation from industrial scale to the custom made laboratory test rig also called CNC-tribometer.

Table 1: Adaptation of process parameters from industrial scale to the laboratory-scale [Olen13a]

Process Parameter	Industry	Tribometer
Number of abrasives, n_{abr}	6	2
Outer diameter, D in mm	540	180
Inner diameter, d in mm	250	60
RPM (ω) in min^{-1}	450	120
Feed rate, v_f in mm/s	75	100
Load in N	1166	102
Abrasive contacts per passage	200	5

The number of abrasive contacts per passage is calculated as a function of tool's geometrical dimensions and process parameters. The intensity of contacts during each passage is represented by this number and can be calculated with the following equation [Olen13a]:

$$N_C = \frac{\pi \cdot (D^2 - d^2) \cdot n_{abr} \cdot rpm}{4 \cdot v_f \cdot D}$$

It can be noted from the data in Table 1 that the number of contact per passage to be undergone by abrasive grinding tools in laboratory scale differ so much from industry. Therefore, more polishing passes (greater polishing time) will be performed on the workpiece in laboratory scale to get significant results in gloss and surface roughness [Olen13a].

In the ceramic tile manufacturing industries, generally more than twenty polishing heads are lined up in sequence to compose an automatic industrial polishing line [Nasc14]. In each polishing head there are grinding tools (also known as fickerts) which were attached on a horizontal spinning plate to keep a radial symmetry position under one polishing head. The process parameters as shown in Table 1 on every polishing tool during the polishing process are kept constant.

It has been reported by several studies that the grinding tools or fickerts move and rotate on their own axes [Hut05b] [Cant04] [Sous07a]. The kinematics behind those motions was studied elsewhere to demonstrate the mathematical equations which deal with the displacement vectors and power per unit time performed during polishing work [Sous07a][Cant04].

Recent evidence by simulation suggests that the contact pressure tends to be 50% higher near to the centre regions worked by the innermost abrasives [Nasc14]. The study had been made according to the calculation and investigation of the grinding work performed due to tribological interaction between porcelain tile and fickerts surfaces [Cant04]. The proposed model was then combined with the kinematics equations of a single rotating abrasive particle with lateral and traversal motions into computational simulation. [Sous07a]

The key explanation of the polishing process parameters are the two different sources of motion in the system. The first motion consists of rotating and downwards pressing polishing head due to its own respective axes with or without traversal movements. The second motion is comprised of the ceramic tile that is laid and fixed firmly on the moving conveyer against the polishing tools (forward motion). This statement explains the origin of surface pressure exerted on the tile surface, which is the normal force from the polishing head, pushing downwards perpendicular to the tile's machined surface. The radial distance of the abrasive blocks from the tool's centre has a significant effect on the tribological interaction in terms of abrasive wear between the outer peripheral of the fickerts and the inner side near to the rotating axis.

This study set out to determine the proposed outcome on the effect of gradual pressure distribution with the presence of helical springs as well as the geometrical variations of both surfaces of fickerts and ceramic tiles in line contact. From previous study made by the author [Sani14], the abraded height of the ceramic tiles shown a very minimum amount of up to 50 μm , while the wear on fickerts is significantly high in millimetre range. The presence of helical springs in the other hand, showed a positive result in terms of greater pressure distribution, greater surface wear, higher gloss level as well as lower surface roughness, which were demonstrated on the machined surface of the ceramic tiles near to its centre.

2.2 Grinding work during polishing

In 2004, Cantavella et al published a paper in which they described the work performed by grinding tools at different points of porcelain tile surfaces [Cant04]. The work executed by the polishing tools was basically divided into three main subjects which are the tool abrasion, the polishing process and other influence factors which contribute mainly to the tribological interactions between fickert and ceramic tile.

In this laboratory case study, the polishing tool consists of two parallelepiped abrasive blocks which are fitted firmly on the tool's holder. By considering the workpiece and the rotating tools in equilibrium as shown in Figure 2-1 below, one can determine the grinding work (dW_p) performed on an element of the tile surface in the time range, $[t+dt]$. Work done on tile surface, dW_p is assumed proportional to the work performed on the fickert element in contact with this surface (dW_m). The work dissipated by other processes (heat transfer, noise, energy dissipation in the grinding machine etc.) is also assumed to be proportional to dW_m analogously. [Cant04]

Mathematically, the relationship of all works performed during polishing of ceramic tiles can be summed up as below:

$$W_{Total} = W_m + W_p + W_{ext}. \quad (2.2)$$

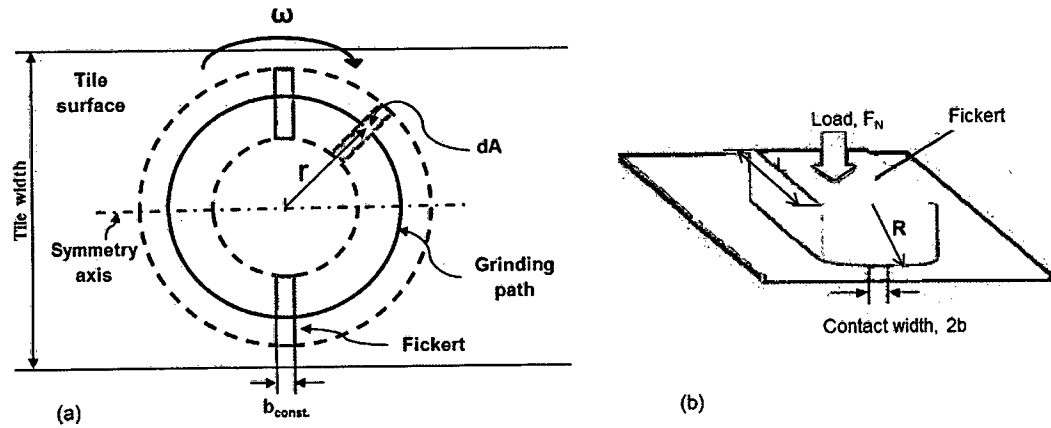


Figure 2-1: Schematic diagrams of: (a) a rotating tangential grinding head with two abrasive blocks attached on it and ceramic tile transported slowly beneath the head (adapted from Cantavella [Cant04]) and (b) a fickert in contact with the tile [Huttc05b]

For a system in equilibrium, the work performed per unit time (power) by the polishing process, $d\dot{W}$ can be calculated from the friction force between the head and the workpiece, which results to the following equation [Cant04]:

$$d\dot{W} = p \cdot \omega \cdot r \cdot \mu \cdot dA \quad (2.3)$$

where:

p is the contact pressure in N/mm²;

ω is the angular speed of the polishing head in rad/s;

r is the distance from the centre of the polishing head to the fickert element in mm;

μ is the coefficient of friction between the abrasive block and the tile surface;

dA is the contact surface between fickert and tile in mm²;

as shown in Figure 2-1.

From Eq. (2.3) above, the abrasive scratching speed in radial distance, v_r is the product of the angular speed and the radius by rotation motion [Nasc14]:

$$v_r = \omega \cdot r \quad (2.4)$$

$$ds = dv_r \cdot dt \quad (2.5)$$

With the rotation motion of the polishing head, a linear variation of velocity against the radius was demonstrated. Cantavella et al [Cant04] had in their work simulated and concluded that, the fickerts abrade equally during the polishing work. They suggested that, the surface of the fickerts is equally abraded and tends to be flat as the region under polishing changes during the polishing process. There is an implication in this argument. The wear of the fickerts across the surface is constant but at particular distance from the rotation

axis, the work done per unit time as suggested by Eq. (2.3) varies with the speed and therefore, by the radius, r . The scratching distance of a particle in radial distance also varies with radius, where the outer particle underwent longer distance than the particle near the rotation axis. The equation of distance travelled, s with its corresponding speed, v_r is given by Eq. (2.5) and (2.4) respectively.

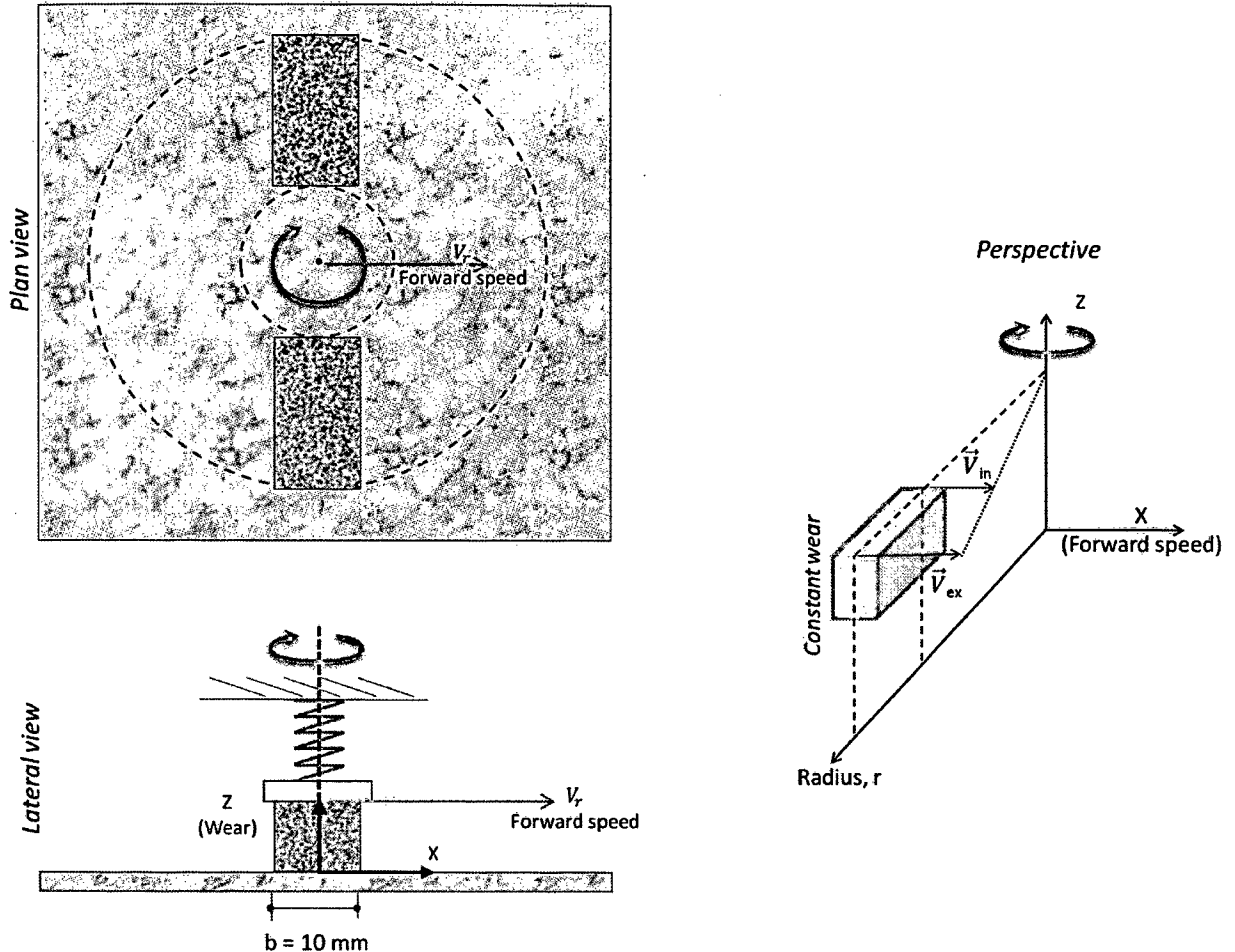


Figure 2-2: Model of the polishing tools, the rotating axis and the corresponding velocity gradient during the polishing process.

For an initial impression, it can be proved by Eq. (2.3) that the polishing power dissipated on the fickerts alone depends on the radial distance to the tool's centre. Throughout this paper the coefficient of friction, normal force and other parameters are assumed constant in the entire grinding surface. Where grinding work is done, there is material removal in terms of abrasive wear, which leads to a proportional correlation between greater grinding work and greater abrasive wear on the fickerts. Therefore, a quantitative laboratory research on the material removal of the rotating fickerts proved that there is a greater wear at the outer side of the radial distance than the side near to the rotation centre of the polishing tool [Sani14] [Glaw12].

Classical theory of abrasive wear was demonstrated by Archard law of wear where the abrasion volume is usually expressed in terms of sliding distance. This law is valid especially for investigations focused on the abrasive pin, which remains continuously exposed to the wear during the tests. [Hutc05b][Sous13b]. In

agreement with the statement, the present work is interested in the distribution of material removal over the ceramic tile sample surface, inside which a linear variation of pressure is demonstrated by the presence of helical springs and acting as the load system normal on the tile surface.

2.3 Spring moment during polishing

The most important discussion in this current work is the surface pressure and its relative speed. They are the most significant influence factors during the polishing process of ceramic tiles to achieve high vitreous effect and fine surface finish. It has come to known so far according to a study by Cantavella et al. that the wear distribution beneath and across the fickers surface is equally distributed [Cant04].

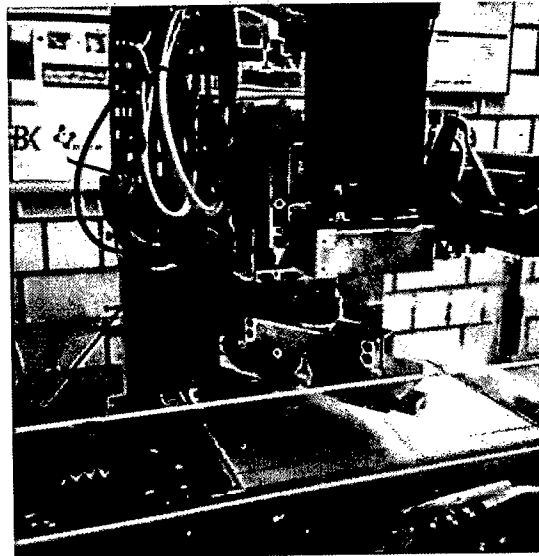


Figure 2-3: Tribometer machine available in the laboratory for the experiments

Preliminary design and construction of the polishing tools to visualize the effect of linear pressure distribution across the surface area was undertaken by Olenburg [Olen14]. The helical spring has been found to oppose the resistance force of the normal load exerted from the tile surface towards the fickers, which then created a linear gradient of pressure distribution from highest to the lowest peak. By highlighting the diagram of a single ficker in equilibrium during the grinding process on the ceramic tile, one could identify the mathematical relations between geometrical changes, the physical as well as mechanical interactions between them.

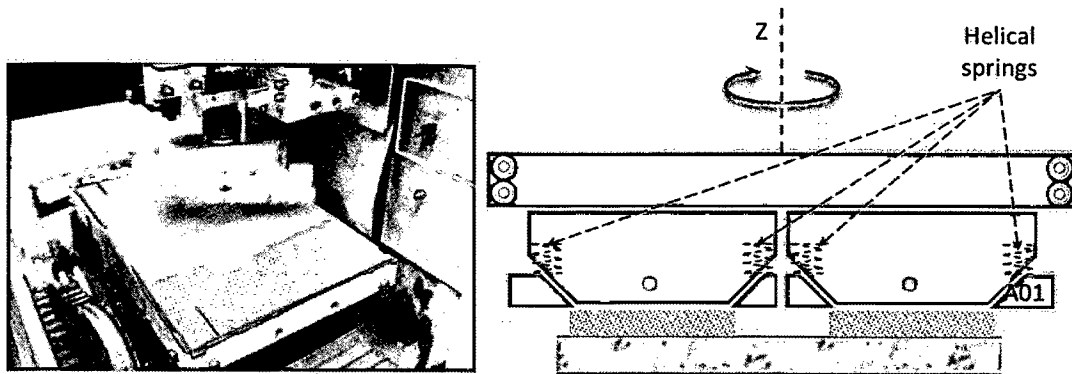


Figure 2-4: Polishing tool in laboratory setup; Right: schematic drawing of the tool

Figure 2-4 above shows a grinding process that took place on the test rig available in the laboratory (Figure 2-3). The schematic drawing in the same figure represents the position of all helical springs mounted on the tool holders during the experiments. Each polishing tool was marked with its own unique identification number and was laser printed on the side surface of the tool's holder (refer Chapter 3.1). A hinge joint interconnects the polishing tool and one tool holder with an abrasive block fitted in it. Due to the normal load acting on the tools and the tools' rotation about the same vertical axis, the loading diagrams of the applied loads and corresponding geometrical changes could be drawn.

As a consequence of a constant normal load pushing downwards, the load's diagram in Figure 2-5 shows the mechanics of grinding process during the rotation of the tools. It is essential to analyse a single grinding tool to better visualise the loading diagram and the after effect of surface wear of both work piece and tools.

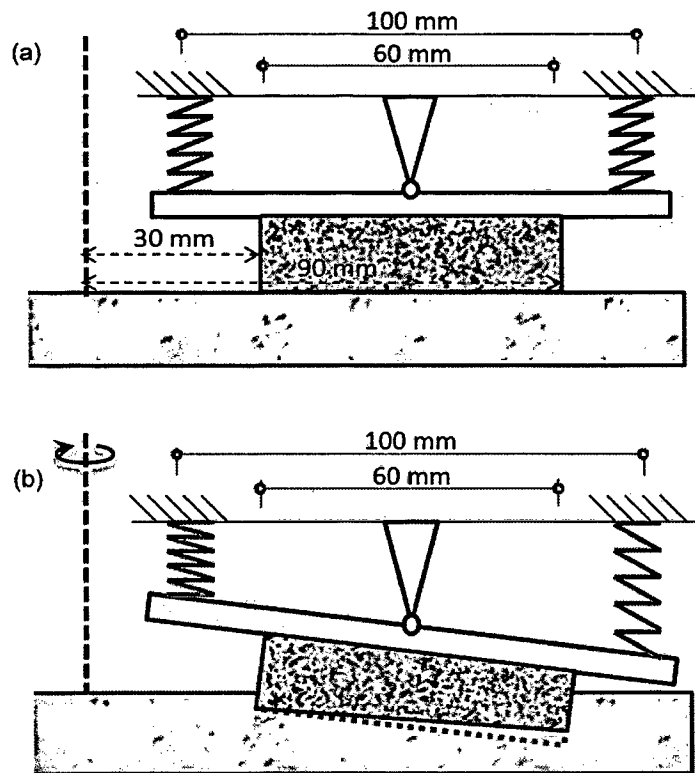


Figure 2-5: Polishing tool (a) at rest and (b) during motion

As shown in Figure 2-5 (b), the effect of more material removal on the farther side of the abrasive from the rotating axis is illustrated. Due to the resisting forces exerted by the spring against the grinding load from the tile surface in the form of compression and elongation of the springs, the abrasive block rotates and the abraded shape remains more at the outer side of the abrasive block than the inner side. This finding is supported by the results presented in the work previously made by the author [Sani14].

From the previous discussion of operating motions in the polishing process system, the force acting on the machined surface of the ceramic tile stems from the normal load acting on the tile surface. The load diagram of the spring pressure exerted against the normal load on the polishing tool is presented in Figure 2-. Despite of rolling free side to side due to the hinge joint, the polishing tools are pressed downwards with both springs' displacements. These displacements are equidistant in different directions. The compression of the spring resulted in more pressure exerted against the tile surface. As a consequence, a higher wear rate of the ceramic tile is to be found on the side near to the tile centre, where the maximum peak pressure is located.

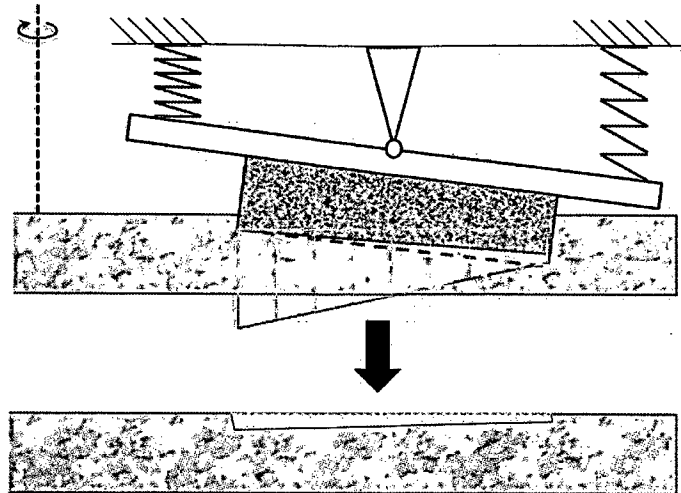


Figure 2-6: Sketch of a loading diagram on the polishing tool and the after effect of abraded surface on the ceramic tile

The force moment about the pivot joint can then be determined by considering all forces acting in the system. The distributed loads on the grinding tools can be calculated with a diagram of motion in static state. This is according to the equation of rigid body and concentrated force in equilibrium.

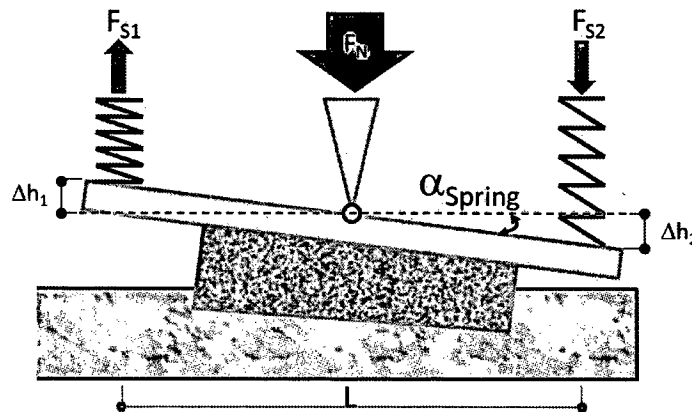


Figure 2-7: Schematic loading diagram of a polishing tool in static state

For the purpose of determining the force moment about the hinge joint, the displacements of the springs and the resultant forces were highlighted in Figure 2-7, where the inclination angle, α_{spring} represents the motion of the forces acted on the pivotal joint. The arctangent of the inclination angle is resulted from the equidistant displacement of the springs. Thus, the distance moved by the springs can be put into a mathematical equation as below:

$$\Delta h_1 = -\Delta h_2 = \Delta h \quad (2.6)$$

The two equal forces in different direction applied equidistant from the hinge joint are the springs' resultant force, F_{spring} , which resists the rotation motion of the tool's holder about the hinge joint, and as a result it will lead to a moment force, M_{Spring} about the joint.

$$F_{S1} = -F_{S2} = F_{Spring} \quad (2.7)$$

Accordingly, the arctangent of the inclination angle is the product of the geometrical changes as shown Figure 2-7 and can be given as:

$$\alpha_{Spring} = \arctan\left(\frac{2 \cdot \Delta h}{L}\right) \quad (2.8)$$

L is the distance between the centre of both springs and Δh is the distance moved by compression/extension of the springs. The inclination angle is very small in relation to the geometrical changes and its value is always lesser than 1°. Thus, it can be expressed with the geometrical changes of the abraded surface alone.

$$\alpha_{Spring} \approx \frac{2 \cdot \Delta h}{L} \quad (2.9)$$

$$\Delta h \approx \frac{\alpha_{Spring} \cdot L}{2} \quad (2.10)$$

The equation of a linear spring under stress is given by Hooke's law, where the force, F_{spring} needed to extend or compress a spring by its displacement, Δh is proportional to that distance. The stiffness factor characteristic to the spring, c_{Spring} , is equal to 20.25 N/mm according to the helical spring manufacturer Febrotec Federn [Febr14].

$$F_{Spring} = c_{Spring} \cdot \Delta h \quad (2.11)$$

Finally the tendency of the tool's holder to move about the hinge joint, also known as force moment by helical spring, M_{spring} , is then given by the product of the resultant force and the proportional distance to the force.

$$M_{Spring} = F_{Spring} \cdot L \quad (2.12)$$

By rearranging equations (2.10) and (2.11) into equation (2.12), the moment force of the springs about the hinge joint is expressed by the following equation:

$$M_{Spring} = \frac{\alpha_{Spring} \cdot c_{Spring} \cdot L^2}{2} \quad (2.13)$$

Equation (2.13) expresses the rotation moment M_{spring} provided by the springs as a function of the inclination angle, α_{spring} , the spring stiffness, c_{spring} , and the distance between the springs, L . The only unknown in this equation, α_{spring} can be derived by measuring the abraded surfaces of both grinding tool and work piece. Figure 2-8 depicts the relationship between both inclined surfaces of the abrasive and the machined surface.

the ceramic tile. Both inclined surfaces are considered as the result of the spring displacement due to material removal during polishing process.

The relation between both inclined surfaces can be equated as:

$$\alpha_{Spring} = \alpha_{Tile} + \alpha_{Abrasive} \quad (2.14)$$

The findings from previous experiments by the author suggest that the inclination angle of the machined surface of the ceramic tile is much lesser than the inclination angle of the abrasive blocks and can therefore be implied as $\alpha_{Tile} \ll \alpha_{Abrasive}$.

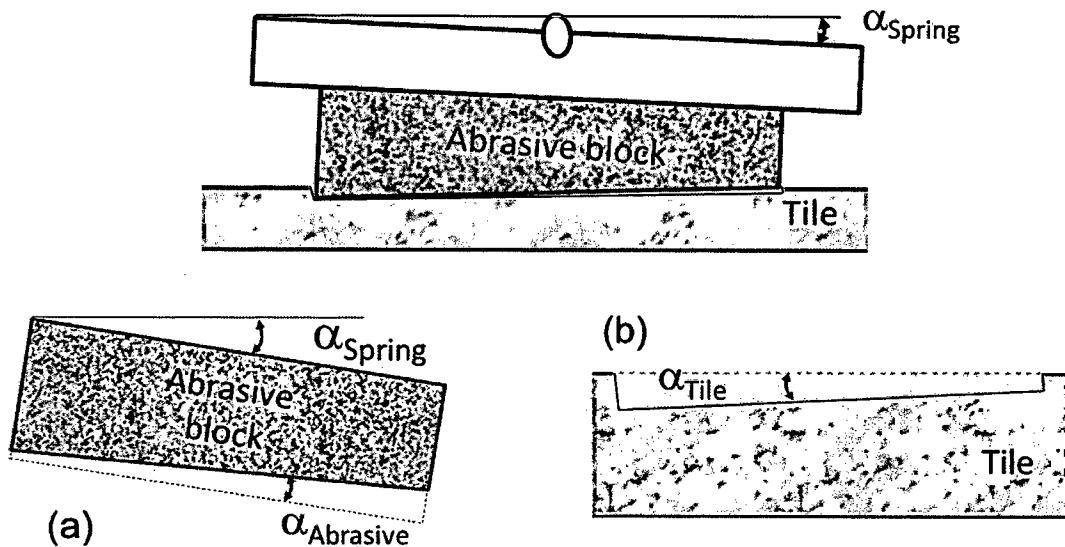


Figure 2-8: Inclination angle of the spring with (a) inclination angle of the abrasive block and (b) inclination angle of the ceramic tile

2.4 Contact Pressure during polishing

The information from previous chapter will be used to develop the equation of spring pressure distribution beneath and across the abrasive surface. It is necessary here to clarify exactly the resulting load acting on the machined surface of the ceramic tile by the abrasive pressure. Figure 2-9 shows the abrasive length, $L_{Abrasive}$ the loading diagram and its equivalence.